Rapid Generation of Block Copolymer Libraries using Automated Chromatographic Separation

Cheng Zhang,^{†,F,I} Morgan W. Bates,[†] Zhishuai Geng,[†] Adam E. Levi,^{†,%} Daniel Vigil,[†] Stephanie M. Barbon,[†] Tessa Loman,[†] Kris Delaney,[†] Glenn H. Fredrickson,^{†,‡,§} Christopher M. Bates,*^{‡,§,%} Andrew K. Whittaker*,^{F,I} and Craig J. Hawker*,^{†,‡,%}

[†]Materials Research Laboratory, [‡]Department of Materials, and [§]Department of Chemical Engineering, [%]Department of Chemistry and Biochemistry, University of California, Santa Barbara, California 93106, United States

¹Australian Institute for Bioengineering and Nanotechnology, ¹ARC Centre of Excellence in Convergent Bio-Nano Science and Technology, University of Queensland, Brisbane, Queensland 4072, Australia

ABSTRACT

A versatile and scalable strategy is reported for the rapid generation of block copolymer libraries spanning a wide range of compositions using a single parent copolymer. This strategy employs automated and operationally simple chromatographic separation that is demonstrated to be applicable to a variety of block copolymer chemistries at multigram scales. The corresponding phase diagrams exhibit increased compositional resolution compared to those traditionally constructed via multiple block copolymer syntheses. Increased uniformity and lower dispersity of the fractionated libraries lead to differences in the location of order—order transitions and observable morphologies, highlighting the influence of dispersity on the self-assembly of block copolymers. Significantly, this chromatographic separation technique greatly simplifies the exploration of block copolymer phase space across a range of compositions and molecular weights and produces more homogeneous materials than conventional synthetic strategies.

INTRODUCTION

Block copolymers (BCPs) find widespread use in fundamental and applied studies due to their self-assembly into a variety of nanoscale morphologies, including various sphere phases, hexagonally-packed cylinders, double gyroid, and lamellae.¹⁻³ A comprehensive understanding of structure–property relationships and the critical agreement between experiment and theory hinges on an accurate assessment of phase behavior, which in the melt state depends on the Flory–Huggins interaction parameter χ , total volumetric degree of polymerization N, relative block volume fractions (e.g., of the A block, f_A), dispersity (D),

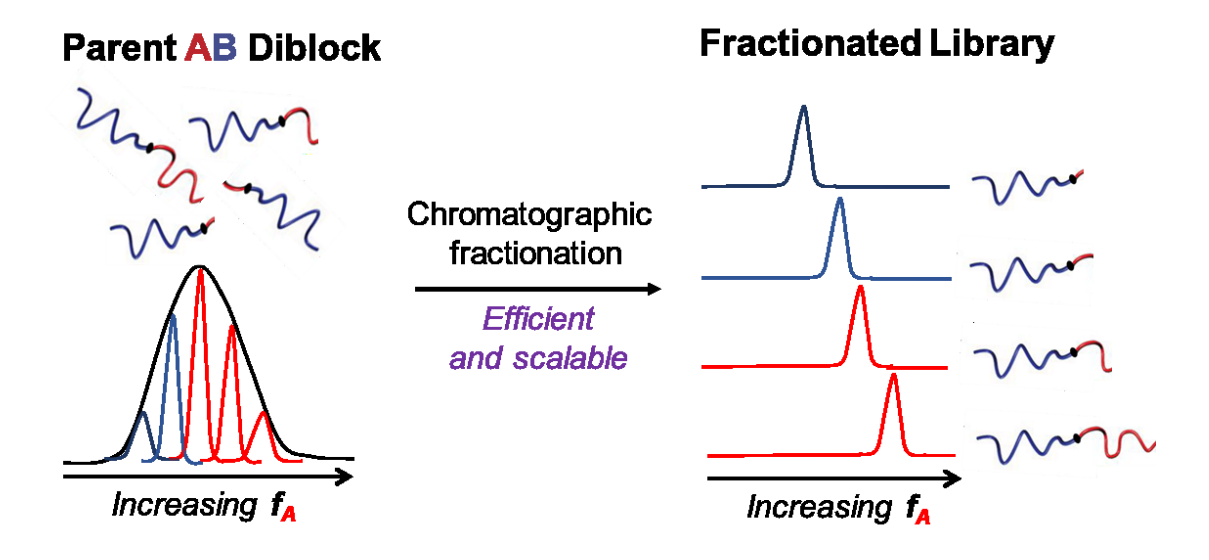
conformational asymmetry, and architecture.⁴⁻⁵ However, the conventional method of exploring phase space is expensive and time consuming, involving the synthesis, purification, and characterization of numerous samples prepared in separate polymerizations targeting a discrete range of compositions.⁵⁻⁷ Issues concerning product uniformity compound these synthetic challenges; for example, subtle differences in molecular weight and composition dispersity for the overall block copolymer and individual domains are known to influence self-assembly and can complicate the interpretation of phase behavior.⁸⁻¹³

To address these challenges and facilitate the exploration of phase space, we describe the use of automated chromatography for the separation of a single BCP starting material into multiple, well-defined samples that span a range of compositions (f_A). This strategy obviates the need to directly synthesize many materials and leads to more uniform dispersity among the sample library. Known collectively as "interaction chromatography" (IC), this separation approach exploits an adsorption-based mechanism that is sensitive to molecular composition of the block copolymer and is tunable by the nature of the column material, temperature, and/or solvent gradients.¹⁴ Pioneering work by Chang demonstrated the feasibility of separating BCPs by composition in one-¹⁴ and two-dimensional¹⁵⁻¹⁶ experiments with the phase behavior of polystyrene-*block*-polyisoprene being examined over a limited range of compositions (\approx 10% in f_A).¹⁷⁻¹⁸ However, the optimization of IC separation conditions is generally not a trivial task and requires complex injection sequences, programmed temperature ramps, and/or the identification of critical conditions to minimize molecular weight effects.¹⁹

In contrast, this report establishes an operationally simpler, automated chromatography technique that can be applied to a wide variety of BCP chemistries and provides scalability for the rapid and precise exploration of phase behavior. Our approach is motivated by recent reports describing the use of automated flash chromatography to fractionate low molecular weight homopolymers into oligomers with discrete chain lengths (D = 1.0). We demonstrate that this technique is applicable to the efficient separation of BCPs into a series of well-defined copolymers of varied composition on multigram scale and relies on basic thin-layer chromatography (TLC) analysis to define the elution conditions (**Scheme 1**). In addition, the fractionation process removes trace quantities of homopolymer to produce BCPs with narrower distributions in molecular weight and average composition than the as-synthesized, parent materials. A comparison of a conventional and a fractionated sample library indicates shifts in order–order and order–disorder phase transitions, highlighting the consequences of dispersity in materials that are otherwise considered fairly monodisperse ($D \le 1.1$). The impetus

of this high-throughput strategy is to facilitate the discovery of structure–property relations in novel BCP materials.

Scheme 1. Chromatographic fractionation of one as-synthesized BCP comprising an inhomogeneous distribution of chains into a series of well-defined fractions that span a range of compositions.



RESULTS AND DISCUSSION

To demonstrate the efficiency of automated chromatography in the exploration of phase space, we initially selected poly(dodecyl acrylate)-block-poly(lactide) (PDDA-b-PLA) as a model diblock copolymer. Its recently reported phase diagram exhibited a rich assembly of spherical morphologies attributed to a large conformational asymmetry parameter quantified by the ratio of block statistical segment lengths, $\varepsilon = b_{\rm PLA}/b_{\rm PDDA} \approx 1.85.^{4,24}$ To outline its phase behavior, this previous study synthesized and examined thirteen individual samples prepared on a multi-gram scale via sequential atom-transfer radical polymerization (ATRP) and ringopening polymerization (ROP). In stark contrast, the automated chromatography technique required a single synthesis of a PDDA-b-PLA diblock copolymer sample ($\langle M_{n,BCP} \rangle = 4000$ g/mol, $\langle f_{PLA} \rangle = 0.34$) (Figures S1 and Table S1).²⁴ Elution conditions appropriate for fractionation were identified from a series of simple TLC experiments and an observable streaking of the sample across the plate (Figure S2). Automated fractionation of the PDDAb-PLA sample (2.5 g) was then completed in under one hour using a hexane/ethyl acetate solvent gradient and a commercial silica chromatography column (Biotage) (Table S2, Figures S3-S4). Figure 1a illustrates the successful fractionation of the starting PDDA-b-PLA copolymer into 20 well-defined BCP samples (10–100 mg each) with an overall mass recovery of 80%. Significantly, ¹H NMR analysis revealed that the fractionated series spanned a broad

compositional window ($f_{PLA} = 0.13-0.48$) derived from BCP starting material with an average composition of $\langle f_{PLA} \rangle = 0.34$ (**Figures 1b** and **S5**). In addition, the separation process readily removed homopolymer impurities, which were present at exceptionally small concentration (ca. 1.0 wt%, see **Figures S6–S7**). This is of particular importance as even small amounts of homopolymer contamination have been shown to impact the phase behavior for a variety of copolymer systems.²⁵⁻²⁶

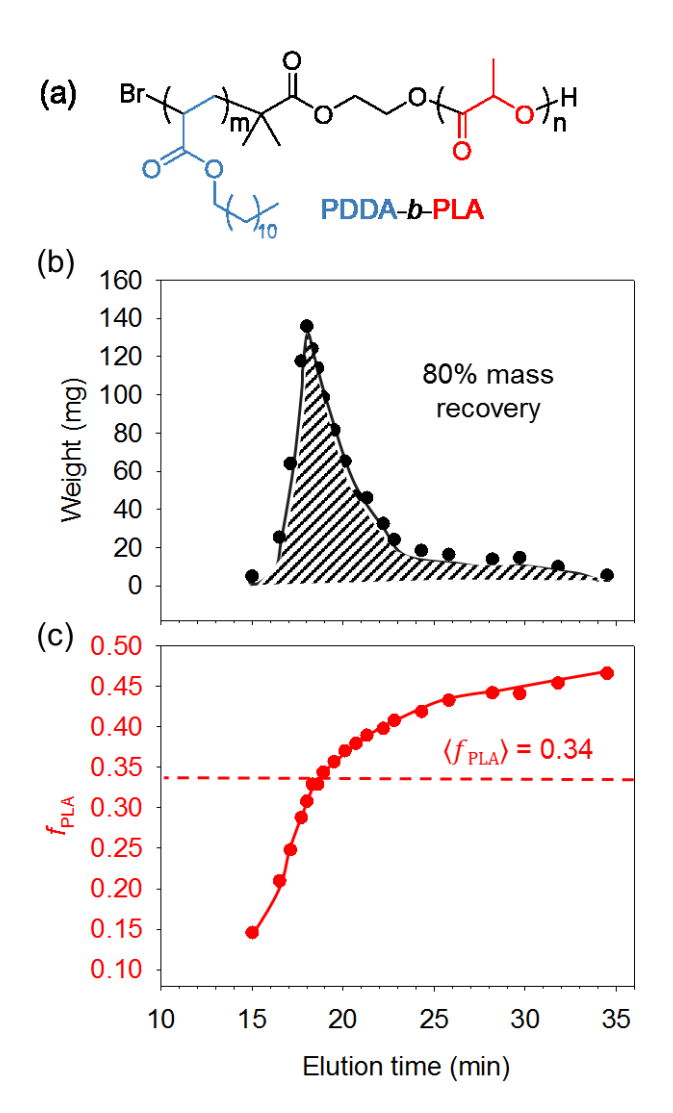


Figure 1. (a) Structure of PDDA-*b*-PLA. Chromatographic separation of a single BCP parent material (2.5 g, $\langle M_{\rm n,BCP} \rangle = 4000$ g/mol, $\langle f_{\rm PLA} \rangle = 0.34$) produces a series of fractionated samples obtained with increasing elution time. A summary of (b) the isolated mass and (c) composition of each fraction ($f_{\rm PLA}$) is depicted. A dashed red line represents the average composition $\langle f_{\rm PLA} \rangle$ of the parent BCP.

The ability to prepare an extensive polymer library from a single parent copolymer is clearly illustrated through the analysis of the fractionated PDDA-b-PLA samples. Changes in

the volume fraction of PLA (f_{PLA}) and molecular weight with elution time quantified using ¹H NMR end-group analysis showed that f_{PLA} increases in a systematic fashion with smaller copolymers (i.e., lower $M_{n,BCP}$) eluting first (**Figure 2a**). This result indicates a separation mechanism involving preferential adsorption between the PLA segment of the polymer and silica gel rather than size exclusion²¹⁻²² since the molar mass of the polar PLA block ($M_{n,PLA}$) continuously increases with elution time while that of the less polar PDDA ($M_{n,PDDA}$) remains relatively constant (**Figure 2b**). Significantly, D of the fractionated BCPs is narrower than the parent BCP (D = 1.10) and decreases from D = 1.08 to 1.05 with each successive fraction (**Figure 2a**).

The efficiency of this process was further demonstrated by taking a fractionated BCP sample ($M_{n,BCP} = 4200 \text{ g/mol}$, $f_{PLA} = 0.35$) and subjecting it to a second fractionation (**Figure S8**). While not as dramatic as the fractionation of the parent material due to the increased uniformity of the starting sample, further segmentation by PLA composition produced an additional library of BCPs across $f_{PLA} = 0.29-0.37$. Consequently, this demonstration suggests that a sequential fractionation technique can enable unprecedented refining to produce high fidelity material libraries across a wide composition range.

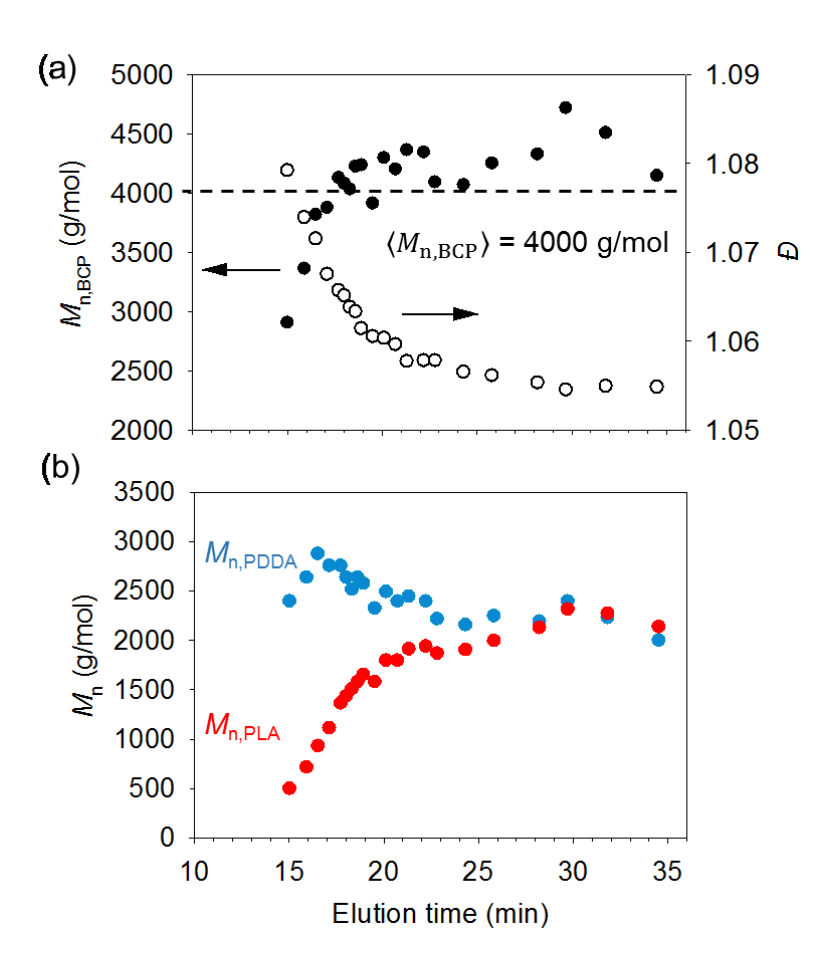


Figure 2. Dependence of (a) $M_{n,BCP}$ and D on elution time following the chromatographic fractionation of a parent PDDA-b-PLA diblock copolymer ($\langle M_{n,BCP} \rangle = 4000$ g/mol, $\langle f_{PLA} \rangle = 0.34$). The dashed black line represents M_n of the parent BCP. (b) The number-average molar mass of the PDDA and PLA blocks in each fraction.

To illustrate that automated chromatography can deliver sufficient quantities of fractionated samples to produce a phase diagram across a range of compositions from a single parent copolymer, 11 of the 20 PDDA-b-PLA fractions were analyzed using variabletemperature small-angle X-ray scattering (SAXS). Significantly, this library results in a comprehensive phase map with a high degree of compositional resolution (Figure 3a and Figure S9) that semi-quantitatively matches the phase diagram obtained via the conventional route (Figure 3b).²⁴ To elucidate the order-disorder phase boundary an estimate of the orderdisorder transition temperature was obtained using SAXS on heating at 10 °C increments (see Figures S10-S11). While the sequence of phases identified in the fractionated library is consistent with past experiments and theory, ²⁴ namely disorder (DIS) → body-centered cubic spheres (BCC) $\rightarrow \sigma \rightarrow A15 \rightarrow$ hexagonally packed cylinders (HEX) as f_A increases from 0.19 to 0.40, there are key reproducible differences in the location of order–order phase boundaries obtained for the two methods (Figures 3b and 3c). In particular, the regions of A15 and σ stability are significantly smaller and better defined after fractionation. We tentatively ascribe this observation to the narrower dispersity in molecular weight and average composition for the fractionated samples. 14,17-19 Preliminary self-consistent field theory (SCFT) calculations confirm that the A15 and σ morphologies are stabilized across narrower compositional windows upon the removal of dispersity (Figure S12). These results are also in agreement with recent insights from Shi et al.²⁷ who proposed the partitioning of chains within micelles of distinct shape and volume as a driver for the stability of various Frank-Kasper sphere phases by reducing packing frustration. A decrease in the degrees of freedom available for monodisperse materials compared to disperse analogues may therefore provide a mechanism to disfavor A15 and σ — with two and five distinct Wyckoff positions, respectively — across larger regions of phase space (Table S3). Further details regarding the SCFT calculations can be found in the Supporting Information.

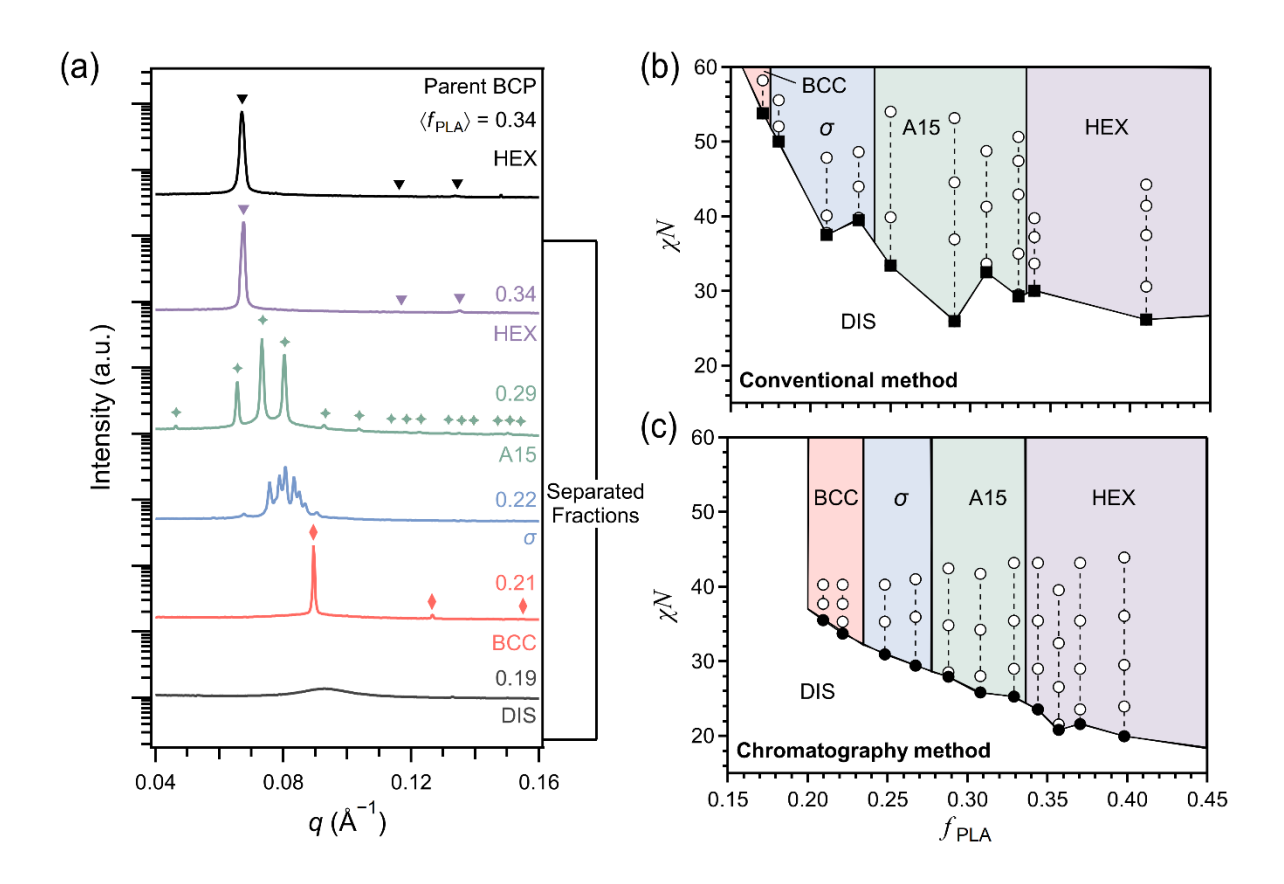


Figure 3. (a) Synchrotron SAXS data of the parent PDDA-*b*-PLA and representative profiles of the fractionated diblock samples of different f_{PLA} . (b) Phase diagrams obtained via a conventional method of individual syntheses (top)²⁴ and the chromatography fractionation method (bottom). Values of $(\chi N)_{\rm ODT}$ are identified by filled symbols. Circles and squares denotes points examined by SAXS and dynamic mechanical thermal analysis, respectively.

The utility of this strategy to examine the consequences of dispersity was further highlighted using other contemporary BCP systems, as demonstrated firstly using poly(dimethylsiloxane)-block-poly(lactide) (PDMS-b-PLA), which has garnered interest as a high- χ , selectively-etch resistant BCP for thin film patterning applications (**Figures 4 and S13–S14**).²⁸ In this case, the as-synthesized PDMS-b-PLA ($\langle M_{n,BCP} \rangle = 9200$ g/mol, $\langle f_{PLA} \rangle = 0.70$, D = 1.08) formed a disordered melt. Significantly, however, upon fractionation, a library of BCPs was obtained that exhibited lamellar order as the f_{PLA} decreased from 0.61 to 0.42. The concomitant change in N of the produced samples resulted in microphase separation at both lower (67) and higher (76) values of χN compared to the parent BCP (73) with the d-spacing undergoing a systematic increase from 9.1 to 10.8 nm as N increases. We attribute these observations to the upward concavity of the order–disorder transition boundary that becomes less steep as f_{PLA} approaches a symmetric composition ($f_{PLA} \rightarrow 0.5$) coupled with the decreased chain dispersity for the

fractionated samples that favors the ordered state. Fractionation of poly(4-*tert*-butylstyrene)-block-poly(methyl methacrylate) (PtBS-b-PMMA, $\langle M_{n,BCP} \rangle = 39300$ g/mol, D = 1.02, $\langle f_{PMMA} \rangle = 0.60$), another high- χ lithographic candidate,²⁹ was similarly performed but primarily governed by column interactions with the PMMA block. Notably, longer range lamellar order was achieved after fractionation, as indicated by the increased scattering intensity and sharper peaks of the fractionated samples relative to the broad reflections of the parent material (**Figures S15–S16**, **Tables S6–S7**).

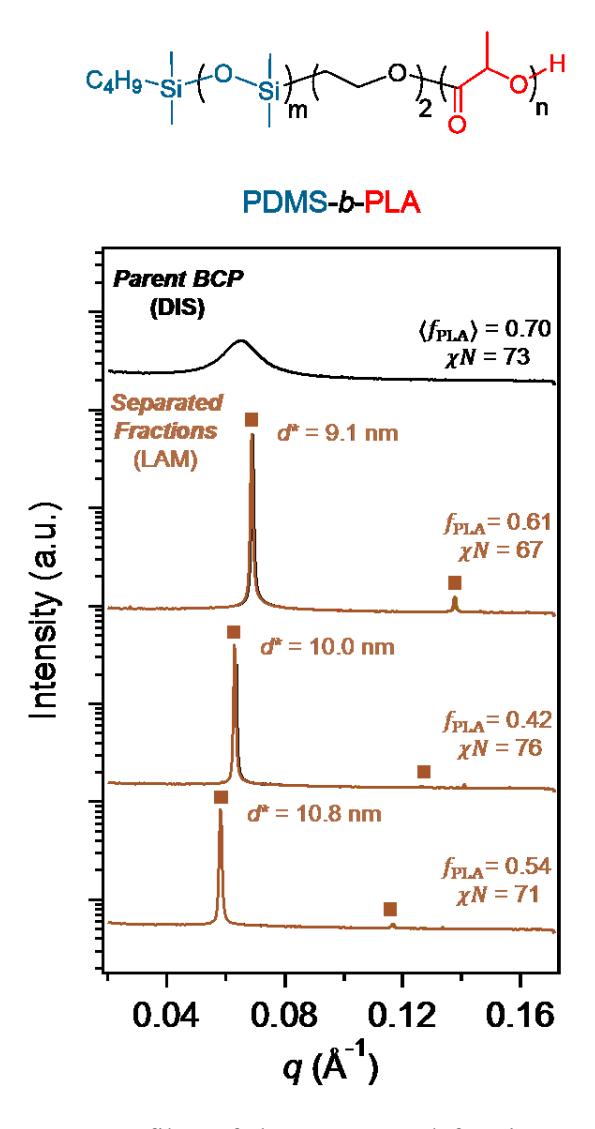


Figure 4. Synchrotron SAXS profiles of the parent and fractionated PDMS-b-PLA diblock copolymers at different f_{PLA} . All SAXS experiments were conducted at room temperature.

Having demonstrated the use of automated chromatography to rapidly prepare phase diagrams and to examine the consequences of dispersity, another key potential advantage of this approach is in the comprehensive survey of systems comprising diverse monomer pairs. This is particularly useful in the context of understanding connections between molecular

design and self-assembly given unprecedented access to new monomer chemistries via contemporary controlled polymerization methods. To illustrate, three previously unreported semi-fluorinated BCPs were examined (**Figure 5**). In each case, the A block was poly(2,2,2-trifluoroethyl acrylate) (PTFEA) while the B block was varied between dodecyl acrylate (DDA), (\pm)menthol acrylate ((\pm)MnA), and dimethyloctanol acrylate (DMOA). The propensity of these combinations to form complex Frank–Kasper sphere phases over minority compositions of the PTFEA block was examined — each B repeat unit includes a bulkier pendant group than the trifluoroethyl-based A block which should increase conformational asymmetry (ε), however the influence of each side-chain on ε and the microphase separation of each system is presently unknown.

The three parent BCPs were prepared with good control over dispersity and molecular weight on multi-gram scale by sequential ATRP polymerization: PTFEA-b-PDDA ($\langle M_{n,BCP} \rangle$ = 8400 g/mol, D = 1.06, $\langle f_{\text{PTFEA}} \rangle$ = 0.31), PTFEA-b-PDMOA ($\langle M_{\text{n,BCP}} \rangle$ = 11700 g/mol, D = 1.06, $\langle f_{\text{PTFEA}} \rangle = 0.27$), and PTFEA-b-P(\pm)MnA ($\langle M_{\text{n,BCP}} \rangle = 14500$ g/mol, D = 1.06, $\langle f_{\text{PTFEA}} \rangle$ = 0.20). The efficient chromatographic fractionation of these semi-fluorinated systems was performed using silica columns and TLC-optimized hexane/ethyl acetate gradients (see the SI for purification and characterization details). A dramatic difference in morphology was observed between the parent copolymer and the corresponding polymer libraries in each case with the SAXS experiments being summarized in Figure 5a-c. The fractionated BCPs exhibit major differences in self-assembly as a function of f_{PTFEA} with PTFEA-b-PDDA copolymers following the sequence: DIS \rightarrow BCC $\rightarrow \sigma \rightarrow$ HEX with increasing f_{PTFEA} (0.15–0.30 was examined with ca. 0.01 composition increments). On the basis of current theory, 6,27 the observation of the σ phase suggests that PTFEA-b-PDDA is a conformationally asymmetric system with $\varepsilon = b_{\text{PTFEA}}/b_{\text{PDDA}} > 1$. This results shows that a survey of phase behavior obtained via fractionation readily enables inherent system properties like conformational asymmetry to be surmised. Furthermore, the high compositional resolution of the sample set enables narrow regions of phase stability (e.g., σ) to be discovered and thoroughly explored. In a similar fashion, PTFEA-b-PDMOA shows BCC and HEX ordered morphologies without observation of the complex spherical σ phase (Figure 5b), indicating the conformational volumes of the blocks are likely closely matched (i.e., $\varepsilon = b_{\text{PTFEA}}/b_{\text{PDMOA}} \approx 1$). Lastly, it is notable that no spherical morphology was observed for the $P(\pm)$ MnA system (**Figure 5c**).²⁴ PTFEA-b- $P(\pm)$ MnA only displays a HEX ordered phase within the explored compositional window, suggesting that the

conformational volume of P(\pm)MnA is likely smaller than that of PTFEA (i.e., $\varepsilon = b_{\text{PTFEA}}/b_{\text{P}(\pm)\text{MnA}} < 1$).

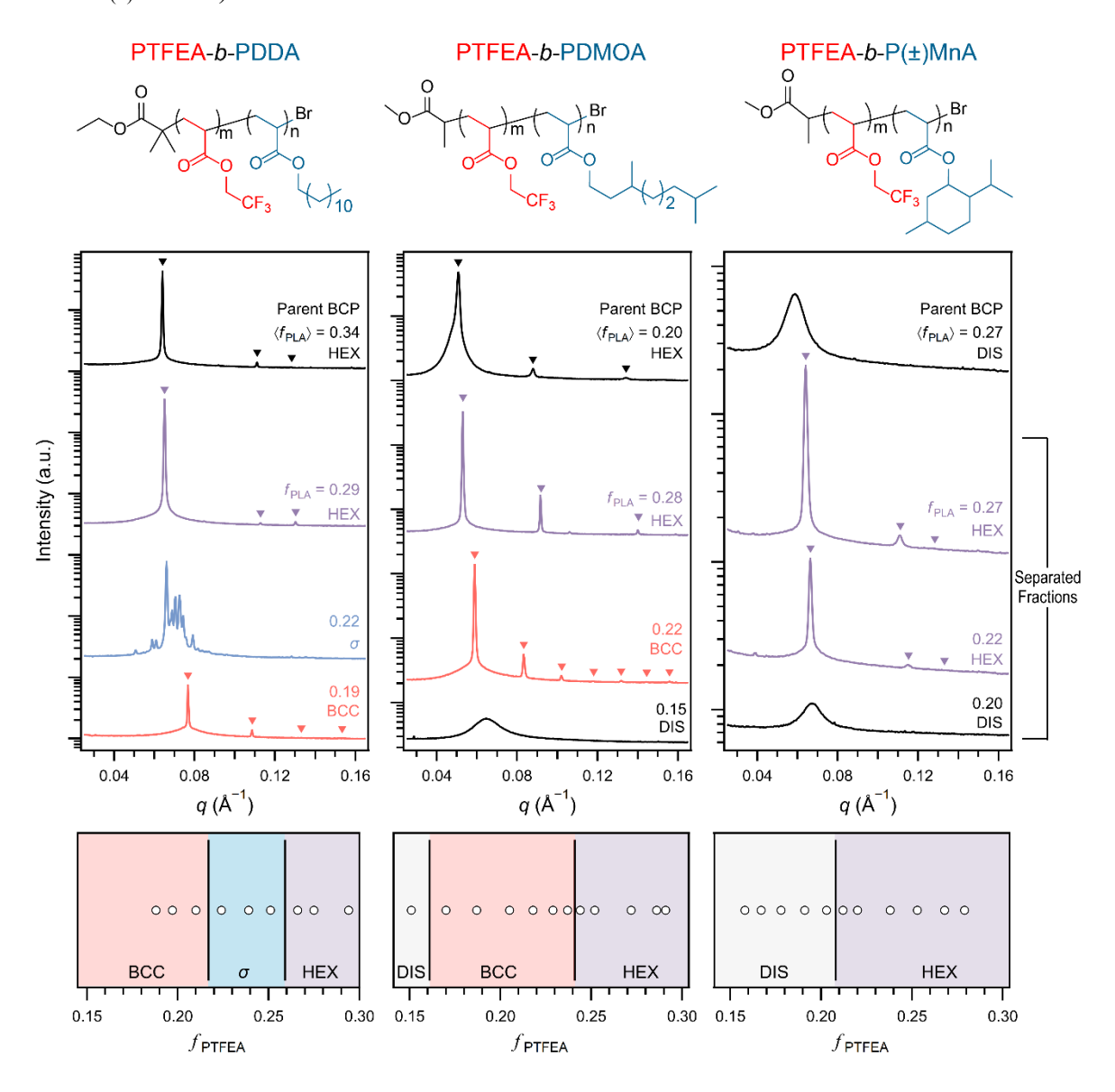


Figure 5. Representative SAXS patterns and a summary of the morphologies found at room temperature for previously unexplored systems of (a) PTFEA-*b*-PDDA, (b) PTFEA-*b*-PDMOA and (c) PTFEA-*b*-P(±)MnA diblock copolymers constructed using the chromatographic separation method.

It is worth noting that the automated chromatography technique is also a tractable for much higher molecular weight BCPs as demonstrated in **Figure S25** using a PTFEA-*b*-PDDA diblock copolymer ($\langle M_{n,BCP} \rangle = 46.3 \text{ kg/mol}$, $\langle f_{PTFEA} \rangle = 0.23$, **Table S14**). Fractionation of the as-synthesized PTFEA-*b*-PDDA was readily achieved using a modified hexane/ethyl acetate solvent gradient optimized based on TLC (**Table S15**). From 3 g of starting material, 15 samples comprising >50 mg were obtained with compositions between $f_{PTFEA} = 0.03-0.33$

(**Figure S25**). The results demonstrate versatility of the automated chromatography to fractionate BCPs over a broad range of molecular weight at multigram scales.

CONCLUSIONS

This report describes an efficient and general strategy for the preparation of BCP libraries based on automated chromatographic separation of a single parent material. Scalable quantities of multiple fractions can be obtained over a wide range of compositions with improved purity and chain dispersity. The technique is shown to be broadly applicable to different monomer chemistries and enables the rapid survey of phase behavior for new BCP systems. Comparisons with traditional polymer libraries produced through individual syntheses of multiple BCPs illustrate important morphological differences. This strategy also quickly enables new insights into the behavior of unknown materials, and it is anticipated that this methodology will dramatically shorten the process of discovery in new and existing BCPs.

ASSOCIATED CONTENT

Supporting Information

Experimental procedures, self-consistent field theory (SCFT) calculations and characterization

data for all block copolymers, including ¹H NMR (Figures S1, S5–S6, S13, S15, S18, S20 and

S22), sample loading and optimization of fractionation (Figures S2-S4), characterization data

and gradient profiles for chromatographic separation (Tables S1-S2 and S4-S15), matrix-

assisted laser desorption/ionization (MALDI) analysis (Figure S7), characterization of a 2nd

fractionation (Figure S8), indexing of the σ phase of PDDA-b-PLA (Figure S9) and PTFEA-b-

PDDA (Figure S24), determination of order-disorder temperature of fractionated PDDA-b-

PLA (Figure S10-S11), SCFT calculations (Figure S12 and Table S3), characterization of

fractioned PDMS-b-PLA (Figure S14), PtBS-b-PMMA (Figures S16–S17), PTEFA-b-PDDA

(Figures S19 and S25), PTFEA-b-PDMOA (Figure S21) and PTFEA-b-P(±)MnA (Figure S23).

This material is available free of charge via the Internet at http://pubs.acs.org.

AUTHOR INFORMATION

Corresponding Authors

*cbates@ucsb.edu

*a.whittaker@uq.edu.au

*hawker@mrl.ucsb.edu

ORCID

Cheng Zhang: 0000-0002-2722-7497

Morgan W. Bates: 0000-0002-8939-2682

Glenn H. Fredrickson: 0000-0002-6716-9017

Christopher M. Bates: 0000-0002-1598-794X

Andrew K. Whittaker: 0000-0002-1948-8355

Craig J. Hawker: 0000-0001-9951-851X

Notes

The authors declare no competing financial interest.

ACKNOWLEDGMENTS

12

The research reported here was primarily supported by the National Science Foundation (NSF) through the Materials Research Science and Engineering Center at UC Santa Barbara, DMR-1720256 (IRG-3). A.K.W. and C.Z. acknowledge support from the Australian Research Council (CE140100036) and National Health and Medical Research Council for an Early Career Fellowship (APP1157440 to C.Z.). M.W.B., A.E.L., and C.M.B. acknowledge the National Science Foundation (award DMR-1844987) for support. Use of the Stanford Synchrotron Radiation Lightsource is supported by the U.S. Department of Energy, Office of Science, Office of Basic Energy Sciences under Contract No. DE-AC02-76SF00515. The SSRL Structural Molecular Biology Program is supported by the DOE Office of Biological and Environmental Research, and by the National Institutes of Health, National Institute of General Medical Sciences (including P41GM103393). The authors thank Dmitriy Uchenik for help with MALDI measurements.

REFERENCES

- 1. Bates, F. S.; Hillmyer, M. A.; Lodge, T. P.; Bates, C. M.; Delaney, K. T.; Fredrickson, G. H., Multiblock Polymers: Panacea or Pandora's Box? *Science* **2012**, *336* (6080), 434-440.
- 2. Kim, H.-C.; Park, S.-M.; Hinsberg, W. D., Block Copolymer Based Nanostructures: Materials, Processes, and Applications to Electronics. *Chem. Rev.* **2010**, *110* (1), 146-177.
- 3. Bates, C. M.; Bates, F. S., 50th Anniversary Perspective: Block Polymers—Pure Potential. *Macromolecules* **2017**, *50* (1), 3-22.
- 4. Bates, M. W.; Barbon, S. M.; Levi, A. E.; Lewis, R. M.; Beech, H. K.; Vonk, K. M.; Zhang, C.; Fredrickson, G. H.; Hawker, C. J.; Bates, C. M., Synthesis and Self-Assembly of ABn Miktoarm Star Polymers. *ACS Macro Lett.* **2020**, *9*, 396-403.
- 5. Shi, L.-Y.; Zhou, Y.; Fan, X.-H.; Shen, Z., Remarkably Rich Variety of Nanostructures and Order—Order Transitions in a Rod—Coil Diblock Copolymer. *Macromolecules* **2013**, *46* (13), 5308-5316.
- 6. Schulze, M. W.; Lewis, R. M.; Lettow, J. H.; Hickey, R. J.; Gillard, T. M.; Hillmyer, M. A.; Bates, F. S., Conformational Asymmetry and Quasicrystal Approximants in Linear Diblock Copolymers. *Phys. Rev. Lett.* **2017**, *118* (20), 207801.
- 7. Yue, K.; Huang, M.; Marson, R. L.; He, J.; Huang, J.; Zhou, Z.; Wang, J.; Liu, C.; Yan, X.; Wu, K.; Guo, Z.; Liu, H.; Zhang, W.; Ni, P.; Wesdemiotis, C.; Zhang, W.-B.; Glotzer, S. C.; Cheng, S. Z. D., Geometry induced sequence of nanoscale Frank–Kasper and quasicrystal mesophases in giant surfactants. *Proc. Natl. Acad. Sci. USA* **2016**, *113* (50), 14195-14200.
- 8. Lynd, N. A.; Hillmyer, M. A., Influence of Polydispersity on the Self-Assembly of Diblock Copolymers. *Macromolecules* **2005**, *38* (21), 8803-8810.
- 9. Widin, J. M.; Schmitt, A. K.; Schmitt, A. L.; Im, K.; Mahanthappa, M. K., Unexpected Consequences of Block Polydispersity on the Self-Assembly of ABA Triblock Copolymers. *J. Am. Chem. Soc.* **2012**, *134* (8), 3834-3844.
- 10. Matsen, M. W., Phase behavior of block copolymer/homopolymer blends. *Macromolecules* **1995**, *28* (17), 5765-5773.

- 11. Huang, Y.-Y.; Hsu, J.-Y.; Chen, H.-L.; Hashimoto, T., Precursor-Driven Bcc–Fcc Order–Order Transition of Sphere-Forming Block Copolymer/Homopolymer Blend. *Macromolecules* **2007**, *40* (10), 3700-3707.
- 12. Wang, S.; Xie, R.; Vajjala Kesava, S.; Gomez, E. D.; Cochran, E. W.; Robertson, M. L., Close-packed spherical morphology in an ABA triblock copolymer aligned with large-amplitude oscillatory shear. *Macromolecules* **2016**, *49* (13), 4875-4888.
- 13. Matsen, M. W., Stabilizing new morphologies by blending homopolymer with block copolymer. *Phys. Rev. Lett.* **1995,** *74* (21), 4225.
- 14. Park, S.; Park, I.; Chang, T.; Ryu, C. Y., Interaction-Controlled HPLC for Block Copolymer Analysis and Separation. *J. Am. Chem. Soc.* **2004**, *126* (29), 8906-8907.
- 15. Lee, S.; Choi, H.; Chang, T.; Staal, B., Two-Dimensional Liquid Chromatography Analysis of Polystyrene/Polybutadiene Block Copolymers. *Anal. Chem.* **2018**, *90* (10), 6259-6266.
- 16. Im, K.; Park, H.-W.; Kim, Y.; Chung, B.; Ree, M.; Chang, T., Comprehensive Two-Dimensional Liquid Chromatography Analysis of a Block Copolymer. *Anal. Chem.* **2007**, *79* (3), 1067-1072.
- 17. Park, S.; Cho, D.; Ryu, J.; Kwon, K.; Lee, W.; Chang, T., Fractionation of Block Copolymers Prepared by Anionic Polymerization into Fractions Exhibiting Three Different Morphologies. *Macromolecules* **2002**, *35* (15), 5974-5979.
- 18. Park, H.-W.; Jung, J.; Chang, T., New characterization methods for block copolymers and their phase behaviors. *Macromol. Res.* **2009**, *17* (6), 365-377.
- 19. Philipsen, H. J. A., Determination of chemical composition distributions in synthetic polymers. *J. Chromatogr. A* **2004**, *1037* (1), 329-350.
- 20. Lawrence, J.; Goto, E.; Ren, J. M.; McDearmon, B.; Kim, D. S.; Ochiai, Y.; Clark, P. G.; Laitar, D.; Higashihara, T.; Hawker, C. J., A Versatile and Efficient Strategy to Discrete Conjugated Oligomers. *J. Am. Chem. Soc.* **2017**, *139* (39), 13735-13739.
- 21. Lawrence, J.; Lee, S.-H.; Abdilla, A.; Nothling, M. D.; Ren, J. M.; Knight, A. S.; Fleischmann, C.; Li, Y.; Abrams, A. S.; Schmidt, B. V. K. J.; Hawker, M. C.; Connal, L. A.; McGrath, A. J.; Clark, P. G.; Gutekunst, W. R.; Hawker, C. J., A Versatile and Scalable Strategy to Discrete Oligomers. *J. Am. Chem. Soc.* **2016**, *138* (19), 6306-6310.
- 22. Oschmann, B.; Lawrence, J.; Schulze, M. W.; Ren, J. M.; Anastasaki, A.; Luo, Y.; Nothling, M. D.; Pester, C. W.; Delaney, K. T.; Connal, L. A.; McGrath, A. J.; Clark, P. G.; Bates, C. M.; Hawker, C. J., Effects of Tailored Dispersity on the Self-Assembly of Dimethylsiloxane–Methyl Methacrylate Block Co-Oligomers. *ACS Macro Lett.* **2017**, *6* (7), 668-673.
- 23. Zhang, C.; Kim, D. S.; Lawrence, J.; Hawker, C. J.; Whittaker, A. K., Elucidating the Impact of Molecular Structure on the 19F NMR Dynamics and MRI Performance of Fluorinated Oligomers. *ACS Macro Lett.* **2018**, *7*, 921-926.
- 24. Bates, M. W.; Lequieu, J.; Barbon, S. M.; Lewis, R. M.; Delaney, K. T.; Anastasaki, A.; Hawker, C. J.; Fredrickson, G. H.; Bates, C. M., Stability of the A15 phase in diblock copolymer melts. *Proc. Natl. Acad. Sci. USA* **2019**, *116* (27), 13194-13199.
- 25. Doise, J.; Bezik, C.; Hori, M.; de Pablo, J. J.; Gronheid, R., Influence of Homopolymer Addition in Templated Assembly of Cylindrical Block Copolymers. *ACS Nano* **2019**, *13* (4), 4073-4082.
- 26. Matsen, M. W., Stabilizing New Morphologies by Blending Homopolymer with Block Copolymer. *Phys. Rev. Lett.* **1995,** *74* (21), 4225-4228.
- 27. Xie, N.; Li, W.; Qiu, F.; Shi, A.-C., σ Phase Formed in Conformationally Asymmetric AB-Type Block Copolymers. *ACS Macro Lett.* **2014**, *3* (9), 906-910.

- 28. Rodwogin, M. D.; Spanjers, C. S.; Leighton, C.; Hillmyer, M. A., Polylactide–Poly(dimethylsiloxane)–Polylactide Triblock Copolymers as Multifunctional Materials for Nanolithographic Applications. *ACS Nano* **2010**, *4* (2), 725-732.
- 29. Kennemur, J. G.; Hillmyer, M. A.; Bates, F. S., Synthesis, Thermodynamics, and Dynamics of Poly(4-tert-butylstyrene-b-methyl methacrylate). *Macromolecules* **2012**, *45* (17), 7228-7236.

For Table of Contents Use Only

Rapid Generation of Block Copolymer Libraries and Phase Diagrams Driven by Automated Chromatographic Separation

Cheng Zhang, Morgan W. Bates, Zhishuai Geng, Adam E. Levi, Daniel Vigil, Stephanie M. Barbon, Tessa Loman, Kris Delaney, Glenn H. Fredrickson, Christopher M. Bates, Andrew K. Whittaker and Craig J. Hawker

